Electronic Supplementary Information of

Generation of Ionic Liquid Tolerant *Pseudomonas putida* KT2440 Strains via Adaptive Laboratory Evolution

Hyun Gyu Lim[a,b], Bonnie Fong[b,g], Geovanni Alarcon[a], Harsha D. Magurudeniya[b,f], Thomas Eng[b,g], Richard Szubin[a], Connor A. Olson[a], Bernhard O. Palsson[a,b,c,d], John M. Gladden[b,e,f], Blake A. Simmons[b,g], Aindrila Mukhopadhyay[b,g,h], Steven W. Singer[b,g], Adam M. Feist[a,b,c,*]

[a]Department of Bioengineering, University of California San Diego, 9500 Gilman Dr., La Jolla, CA 92093, USA

[b]Joint BioEnergy Institute, 5885 Hollis street, 4th floor, Emeryville, CA 94608, USA

[c]Novo Nordisk Foundation Center for Biosustainability, Technical University of Denmark, 2800 Kgs, Lyngby, Denmark

[d]Department of Pediatrics, University of California, San Diego, CA 92093, USA

[e]Department of Energy, Agile BioFoundry, Emeryville, CA 94608, USA.

[f]Department of Biomass Science and Conversion Technology, Sandia National Laboratories, 7011 East Ave, Livermore, CA 94550, USA

[g]Biological Systems and Engineering Division, Lawrence Berkeley National Laboratory, 1 Cyclotron Road, Berkeley, CA 94702, USA

[h]Environmental Genomics and Systems Biology Division, Lawrence Berkeley National Laboratory, 1 Cyclotron Road, Berkeley, CA 94702, USA

*To whom correspondence should be addressed.

(Adam M. Feist)

afeist@ucsd.edu

Supplementary Text 1. Speculations for impacts of mutations in the condition-specific 'key-3' regions

Various mutations on *relA* (PP_1656 encoding ATP:GTP 3'-pyrophosphotransferase) gene were detected in all 16 lineages regardless of the experimental conditions, indicating that this gene is critical for the adaptation to the medium (Fig. 3 and Table 1). Even though mutation patterns were dynamically changing during the evolution, many mutations were loss-of-function mutations such as altered start codon, insertion of early stop codons, frameshift mutations (Fig. S7a). Given that *relA* is responsible for synthesizing (p)ppGpp (guanosine pentaphosphate or tetraphosphate) which is an alarmone inducing the stringent response in microorganisms when amino acid starvation occurs,[1] it was believed that reduction of the stress signal is beneficial for higher growth rates and biomass formation. Indeed, it was observed that the deletion of *relA* significantly increased the growth rate of *Salmonella Typhimurium*.[2] Interestingly, despite the high frequency observed in this study, mutations on *relA* were not observed in a previous KT2440 evolution study[3] which was conducted under a similar condition. We found that initial strains have different genotypes (including G203D of *relA*) even though those are known as the same KT2440 strain (Supplementary Data 1); this initial different genetic background might attribute to such difference.

oprB-II (PP_1445 encoding a carbohydrate-selective porin) and the intergenic region with PP_1446 (encoding TonB-dependent receptor) were also frequently mutated in seven different lineages across two different experimental conditions (control and [TEOH][OAc]). OprB-II is known to be related to the uptake of glucose[4] whereas the role of PP_1446 has not been identified. Interestingly, two mutations in the gene are synonymous, which would maintain the activity of OprB-II, and located at the middle or end of the protein (at the 265th and 384th

amino acids of 444 total amino acids) (Fig. S7b). One interpretation of the adaptation mechanism is that the mutations increased the expression of *oprB*-II gene or downstream *gcd* gene (PP_1444 encoding quinoprotein glucose dehydrogenase) that could lead to an improvement in glucose utilization by changing the activities of their promoter regions.

fleQ (PP_4373 encoding a transcriptional regulator controlling the flagella synthesis) was also commonly mutated in the 4 lineages of the control experiment. In accordance with previous observations,[3,5] *fleQ* was inactivated in most evolved strains from the control experiment by the insertion of stop codons or frame-shift mutations (Fig. S7c). The inactivation probably is for avoiding unnecessary generation of the flagella under the well-mixed experimental condition.[6,7]

Mutation events in *tktA* (PP_4965 encoding transketolase A) introduced several non-synonymous changes and an insertion of amino acids (Fig. S7d) in 3 lineages of the control experiment. TktA catalyzes the interconversion of glyceraldehyde-3-phosphate (G3P) and sedoheptulose-7-phosphate (S7P) into ribose-5-phosphate (R5P) and xylulose 5-phosphate (X5P). Although it is an important gene related to glucose metabolism, their effects on the activity of TktA are currently not clear, given that there are many peripheral pathways in KT2440.[8]

Mutations on *gacS* (PP_1650 encoding a sensor protein) were observed in 7 lineages of the TALEs (Table S3 and Supplementary Data 2). However, this gene was classified as the medium-specific regions (Fig 3), g.iven that mutations on *gacS* have been observed in other evolution studies[3,7] not related to the IL. It is known that GacS consists of a two-component system with GacA (also known as UvrY), controlling genes related to the biofilm formation; the deletion of *gacS* adversely affected the biofilm formation.[9,10] As many mutations are insertions of stop codons or frame-shift mutations (Fig. S7e), the cells have been evolved not to synthesize

unnecessary biofilm similar to the *fleQ* case. Indeed, it was shown that the deletion of *gacS* improves the growth rate of *Pseudomonas* sp. PCL1171.[11]

Similarly, *uvrY* (PP_4099 encoding a BarA(GacS)-UvrY two-component system response regulator)-PP_4100 (encoding a Cro-CI family transcriptional regulator) region was also classified as the medium-specific regions (Fig. 3), although its mutations were observed in three different TALE experiments regardless of the IL (Fig. S7f, Supplementary Data 2). On the contrary to *gacS* that mostly acquired the loss-of-function mutations, the mutations of UvrY are a duplication of 27-bp, a single amino acid change, a base pair change in its 5'-untranslated region. Currently, the reason is not clear, further studies would be informative to understand the effect of the mutations.

Supplementary Text 2. Speculations for impacts of mutations in the IL-specific 'key-3' regions

Two different in-frame deletion mutations (42-bp and 69-bp) of *oprD* (PP_1206) encoding outer membrane basic amino acid-specific porin were observed in the 4 lineages of the [TEA][HS] tolerization ALE (TALE9-12, Fig. S7g). However, only the 69-bp-deletion mutation was fixed in two end-point strains (Supplementary Data 2). It is reported that OprD facilitates uptake several antibiotics such as imipenem although it mainly imports basic amino acids.[4,12] Although it is not clear, OprD might be acted as a channel for the entering of [TEA][HS] and the cell achieved the tolerance by decreasing the size of OprD causing a loss of the import activity.

One identical synonymous mutation (G38G) in the PP_5324 gene encoding a two-component system response regulator was observed (Fig. S7h) in three different lineages of the TALE experiments that used [TEOH][OAc]. Although this gene was classified as an IL-specific region because its mutation has not been observed in any other studies, this gene may be related to general stress response and the flagella synthesis; two previous studies reported that its gene expression was changed under an elevated pressure condition (i.e., high oxygen concentration condition)[13] or with the deletion of *fliA* (PP_4341 encoding the RNA polymerase sigma 28 factor)[14] which is closely related to the flagella synthesis. The expression of PP_5324 was co-regulated with *gacS*, *cheA* (encoding a chemotaxis histidine kinase), *cheZ* (encoding a protein phosphatase).[15]

Supplementary Figures

Fig. S1. Initial evaluation of ionic liquid (IL) toxicities to the wild-type *Pseudomonas putida* KT2440 (KT2440) strain

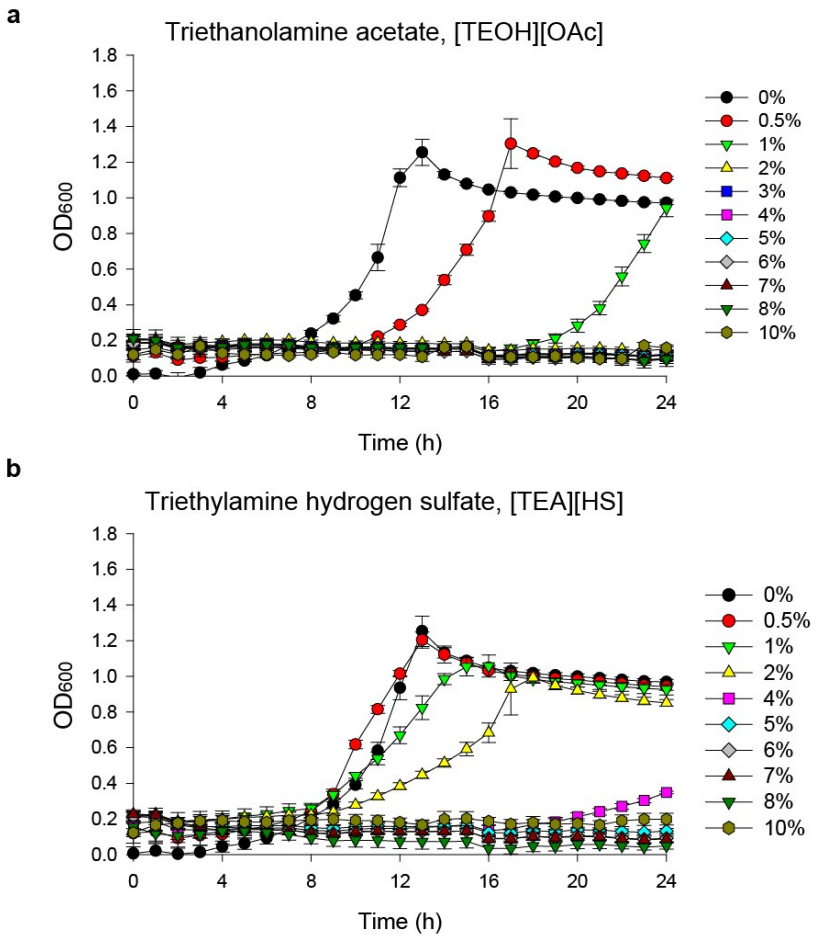

Growth profiles of KT2440 in the presence of various concentrations (% w/v) of (a) triethanolammonium acetate ([TEOH][OAc]), (b) triethylammonium hydrogen sulfate ([TEA][HS]) in 200 µL of the medium. Error bars indicate the standard deviation of three independent cultures (n=3). The x-axis and y-axis indicate time (h) and optical density at 600 nm (OD_{600}), respectively.

Fig. S2. Differentially expressed genes (DEGs) by the addition of ILs.

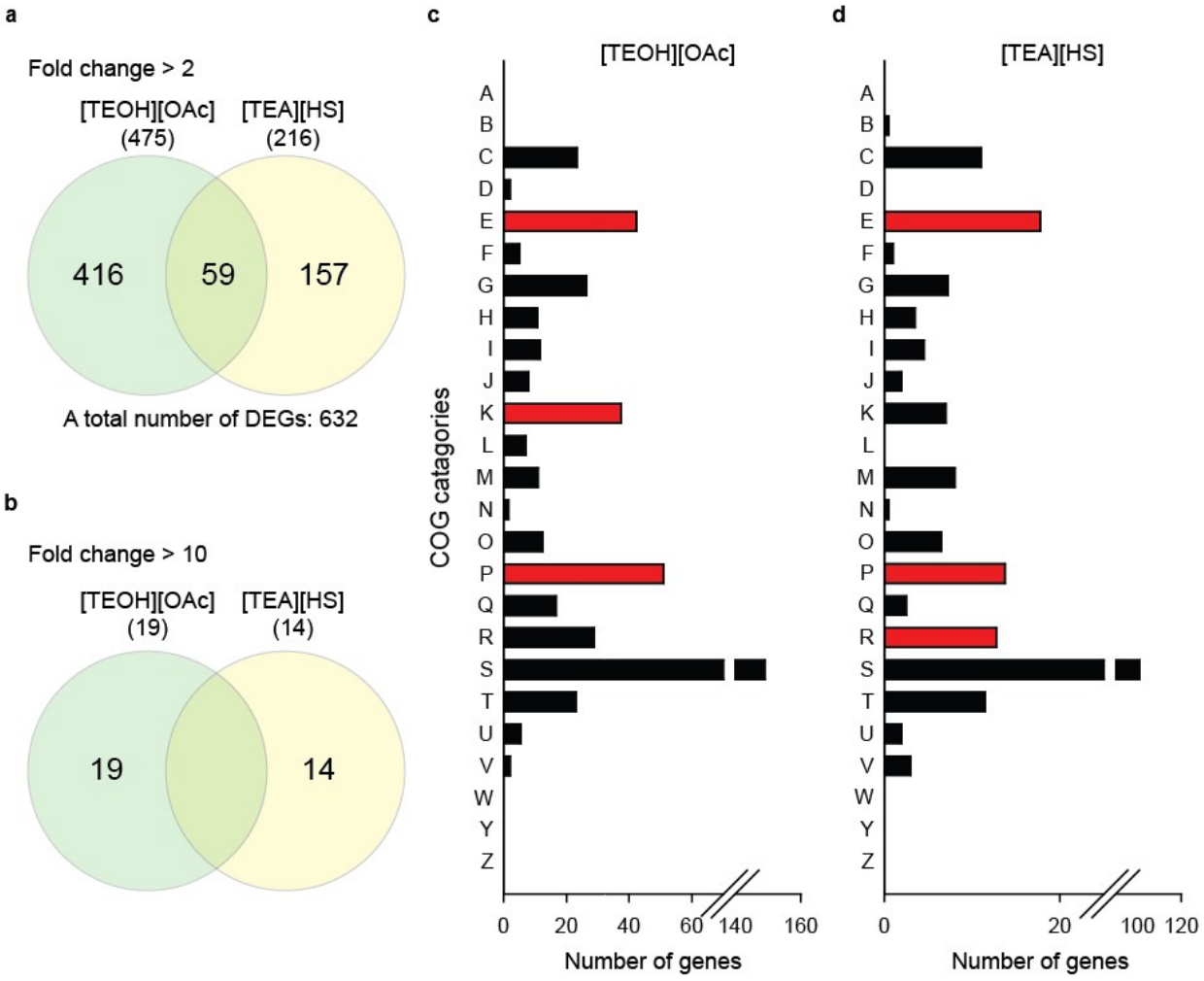

(a-b) Venn diagrams indicating numbers of DEGs upon the addition of [TEOH][OAc] and [TEA][HS]. Either 0.5% w/v [TEOH][OAc] or 2% w/v [TEA][HS] was added in the modified M9 medium. Fold changes are greater than (a) 2 or (b) 10. (c-d) Categorized DEGs (fold changes > 2) into clusters of orthologous groups (COGs) based on annotated functions. (c) [TEOH][OAc] and (d) [TEA][HS] were added. Red-colored bars indicated the top 3 groups in each condition except the category [S], unknown function. Other category symbols: A, RNA processing and modification; B, chromatin structure and dynamics; C, energy production and conversion; D, cell cycle control and mitosis; E, amino acid metabolism and transport; F, nucleotide metabolism and

transport; G, carbohydrate metabolism and transport; H, coenzyme metabolism; I, lipid metabolism; J, translation; K, transcription; L, replication and repair; M, cell wall/membrane/envelop biogenesis; N, cell motility; O, post-translational modification, protein turnover, chaperone functions; P, inorganic ion transport and metabolism; Q, secondary structure; R, general functional prediction only; T, signal transduction; U, intracellular trafficking, secretion, and vesicular transport; V, defense mechanism; W, extracellular structure; Y, nuclear structure; Z, cytoskeleton. All unannotated genes were manually assigned in the category [S].

Fig. S3. Trajectories of the control ALE experiments without the stress

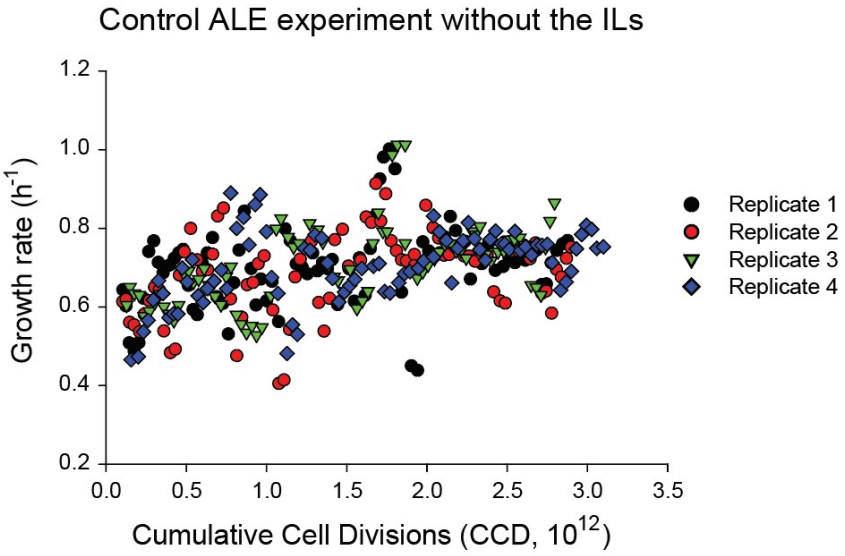

The control ALE experiment without the ILs was conducted with 4 biological replicates. The final average growth rate of 4 different lineages was 0.79 h^{-1} while the initial average growth rate was 0.58 h^{-1}. The left *y*-axis indicates the growth rate of each population. Each growth rate has been averaged with the values of 3 consecutive flasks (one before and after) because of fluctuation in growth rate measurement arisen from inappropriate sampling intervals, dust on wells of OD-measurement plates, etc.

Fig. S4. Evaluation of IL tolerance of the end-point strains with different concentrations of [TEOH][OAc]

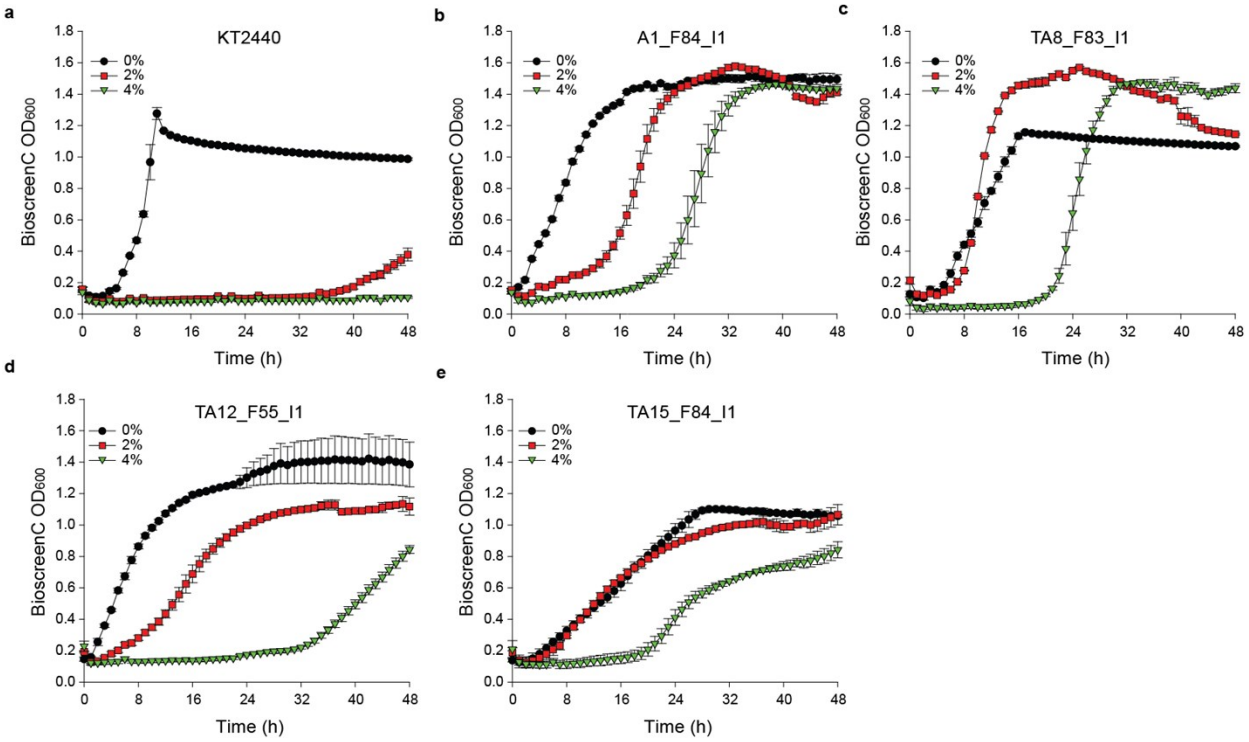

(a-e) Growth profiles of (a) the KT2440 and the best end-point strains (b-A1_F84_I1, c-TA8_F83_I1, d-TA12_F55_I1, e-TA15_F84_I1) showing highest growth rates with 4% [TEOH][OAc] from the same experimental conditions. The *x*-axis and *y*-axis indicate time (h) and optical density at 600 nm (OD_{600}), respectively. Error bars indicate the standard deviation of three independent cultures (*n*=3). Symbol: black circle, 0%; red square, 2%; green down triangle, 4%

Fig. S5. Evaluation of IL tolerance of the end-point strains with different concentrations of [TEA][HS]

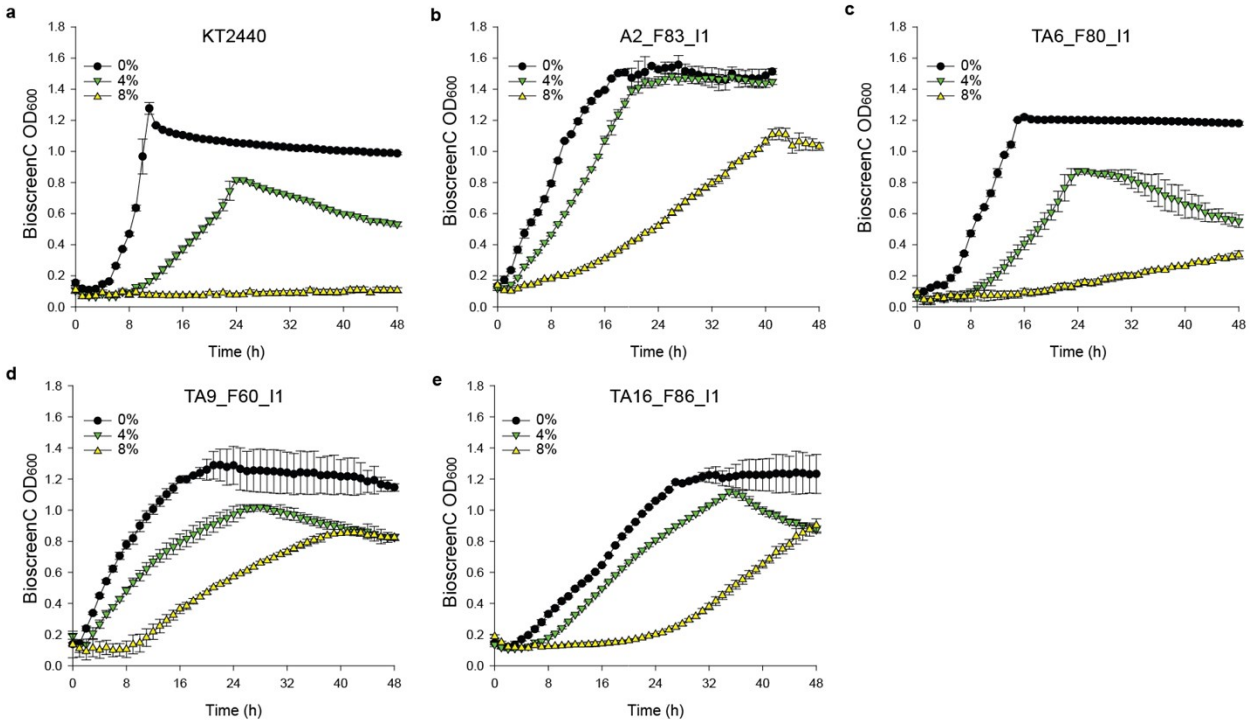

(a-e) Growth profiles of (a) the KT2440 and the best end-point strains (b-A2_F83_I1, c-TA6_F80_I1, d-TA9_F60_I1, e-TA16_F86_I1) showing highest growth rates with 8% [TEA][HS] from the same experimental conditions. The *x*-axis and *y*-axis indicate time (h) and OD_{600}, respectively. Error bars indicate the standard deviation of three independent cultures (*n*=3). Symbol: black circle, 0%; green down triangle, 4%; yellow up triangle, 8%

Fig. S6. Growth rate comparison of the wild-type strain and the end-point strains from the control ALE experiments

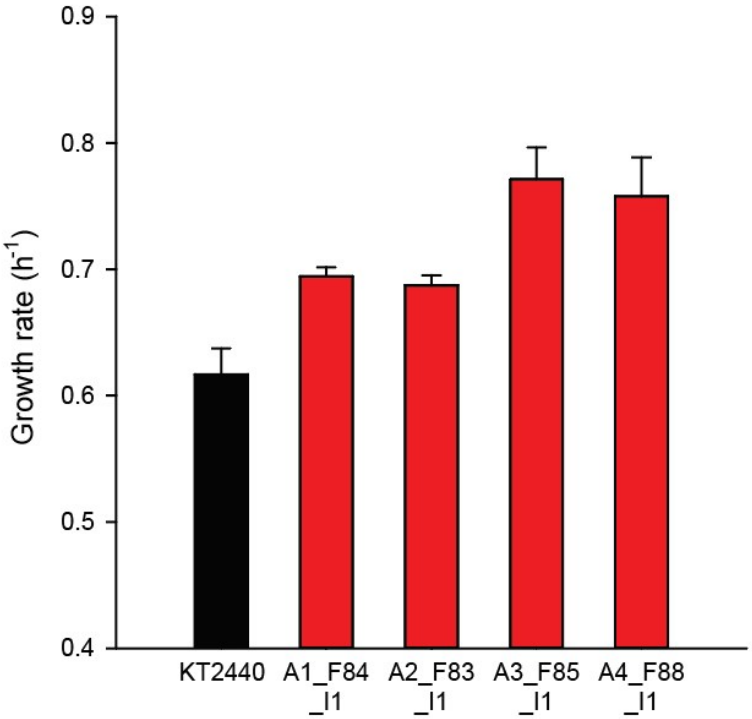

The *y*-axis indicates the maximum specific growth rate (h^{-1}). Error bars indicate the standard deviation of three independent cultures (*n*=3).

Fig. S7. Mutations on the genomic regions in the evolved strains

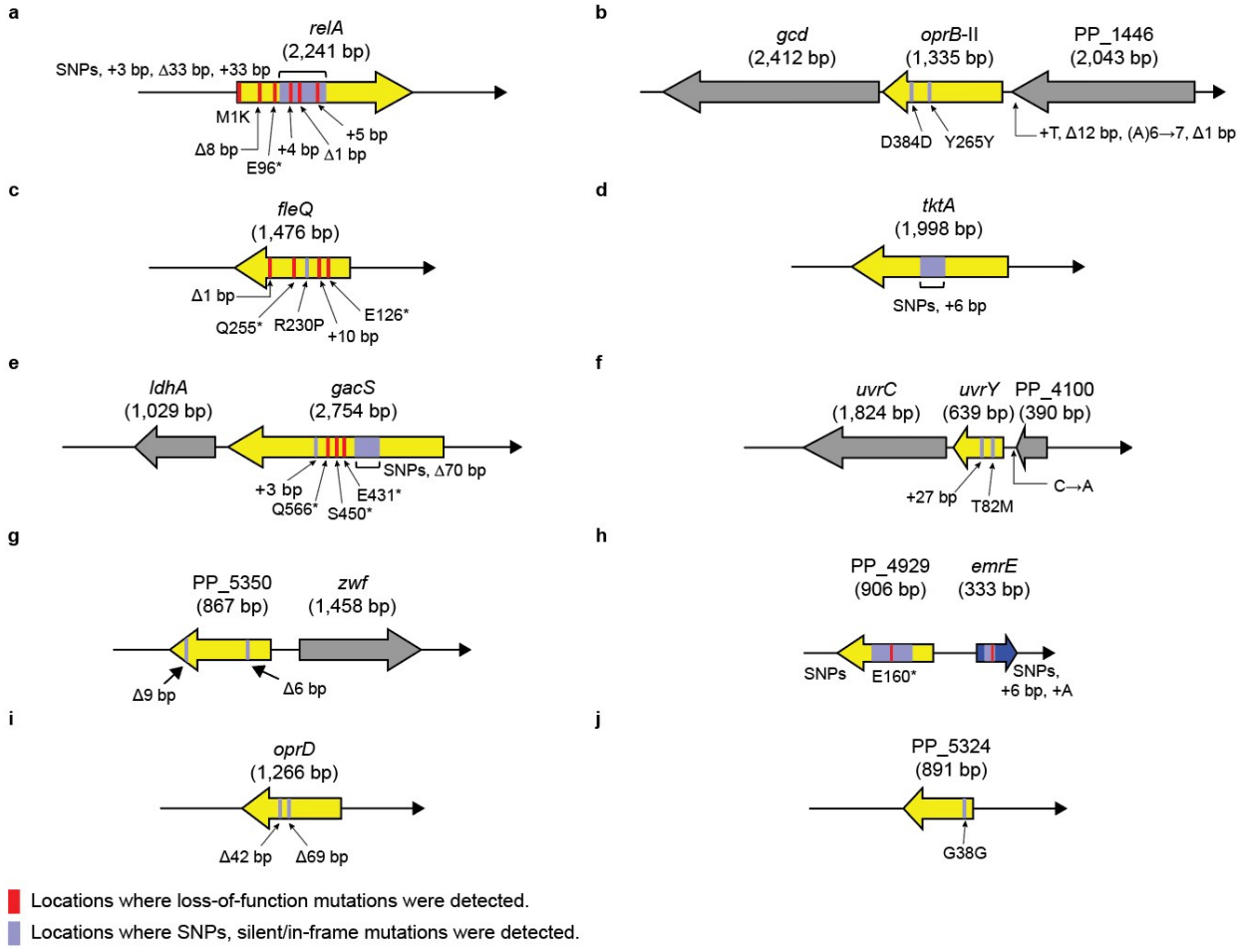

Mutations observed in the evolved strains were depicted (a-j). (a) *relA* encodes ATP:GTP 3'-pyrophosphotransferase (b) *gcd, oprB*-II, and PP_1446 encode quinoprotein glucose dehydrogenase, carbohydrate-selective porin, and TonB-dependent receptor (c) *fleQ* encodes a transcriptional regulator (d) *tktA* encodes transketolase (e) *ldhA* and *gacS* encode D-lactate dehydrogenase and sensor protein (f) *uvrC* and *uvrY* encode UvrABC system protein C and BarA-UvrY two-component system response regulator. PP_4100 encodes Cro-CI family transcriptional regulator. (g) PP_5350 and *zwf* encode RpiR family transcriptional regulator and glucose 6-phosphate 1-dehydrogenase (h) PP_4929 and *emrE* encode LysR family transcriptional regulator and small multidrug resistance protein (i) *oprD* encodes basic amino

acid specific porin. (j) PP_5324 encodes a two-component system response regulator. Arrows indicate direction of the genome. Red-colored regions indicate loss-of-function mutations such as altered stop codon, early termination, frameshift. Regions showed SNPs, silent or in-frame mutations were colored as purple. All detailed mutations are listed in Supplementary Data 2.

Fig. S8. Sequence alignment of EmrE in *P. putida* KT2440 and *E. coli* K-12 MG1655.

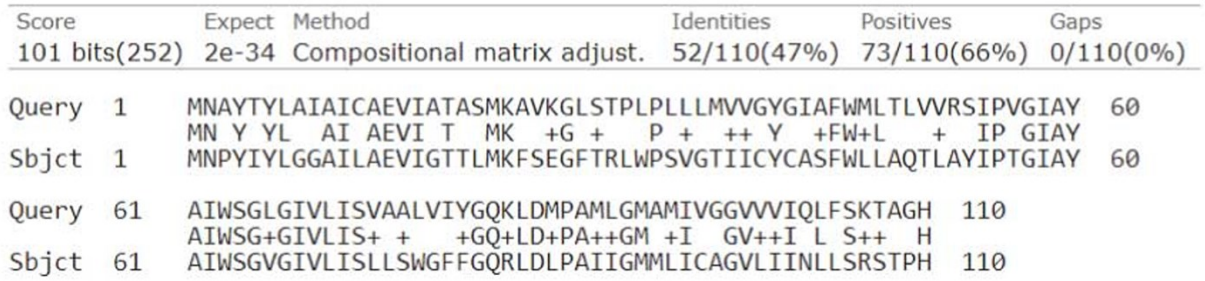

Score	Expect	Method	Identities	Positives	Gaps
101 bits(252)	2e-34	Compositional matrix adjust.	52/110(47%)	73/110(66%)	0/110(0%)

```
Query  1    MNAYTYLAIAICAEVIATASMKAVKGLSTPLPLLLMVVGYGIAFWMLTLVVRSIPVGIAY  60
            MN Y YL  AI AEVI T  MK  +G +   P +  ++ Y  +FW+L   +  IP GIAY
Sbjct  1    MNPYIYLGGAILAEVIGTTLMKFSEGFTRLWPSVGTIICYCASFWLLAQTLAYIPTGIAY  60

Query  61   AIWSGLGIVLISVAALVIYGQKLDMPAMLGMAMIVGGVVVIQLFSKTAGH  110
            AIWSG+GIVLIS+ +   +GQ+LD+PA++GM +I  GV++I L S++  H
Sbjct  61   AIWSGVGIVLISLLSWGFFGQRLDLPAIIGMMLICAGVLIINLLSRSTPH  110
```

The query sequence is the amino acid sequence of EmrE in the KT2440 strain and the subject (Sbjct) sequence is the amino acid sequence of EmrE in *E. coli* K-12 MG1655.

Fig. S9. Growth dependency of the wild-type KT2440 and TA8_F83_I1 strain to acetate

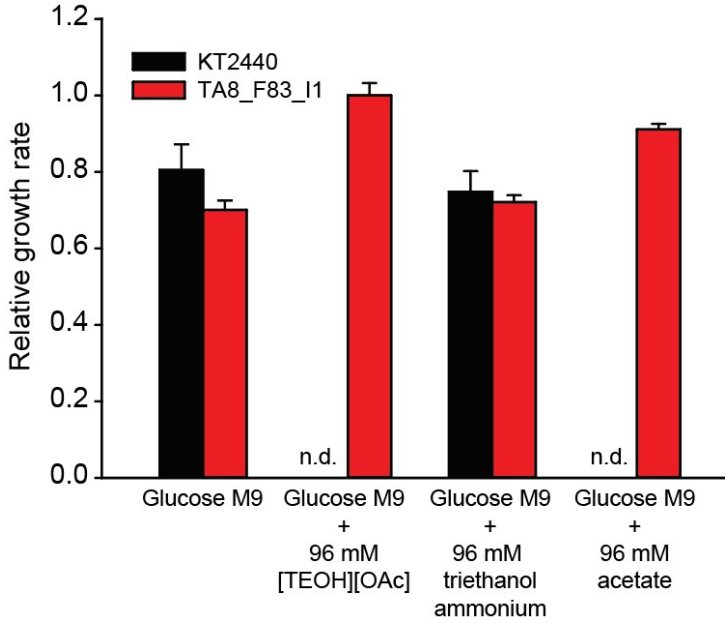

Relative growth rates of wild-type KT2440 and TA8_F83_I1 strains in 200 μL of the medium depending on additional supplementation of 96 mM (2% w/v) [TEOH][OAc] or the equimolar concentration of each component. Triethanolamine and acetic acid were neutralized to pH 7 by the addition of hydrochloric acid and sodium hydroxide, respectively. The cultivation was monitored for 24 h. All growth rates are normalized values by the growth rate of the TA8_F83_I1 strain with 96 mM [TEOH][OAc]. Error bars indicate the standard deviation of three independent cultures (n=3). N.d.: no detectable growth.

Supplementary Tables

Table S1. Strains and plasmids used in this study

Name[a]	Description[b]	Source
Strains		
KT2440	Wild-type *Pseudomonas putida* KT2440	ATCC 47054
E. coli S-17	A host for the conjugation	ATCC 47055
A1_F84_I1	An isolate from ALE lineage 1	This study
A2_F83_I1	An isolate from ALE lineage 2	This study
A3_F85_I1	An isolate from ALE lineage 3	This study
A4_F88_I1	An isolate from ALE lineage 4	This study
TA5_F91_I1	An isolate from TALE lineage 5	This study
TA6_F80_I1	An isolate from TALE lineage 6	This study
TA7_F80_I1	An isolate from TALE lineage 7	This study
TA8_F83_I1	An isolate from TALE lineage 8	This study
TA9_F60_I1	An isolate from TALE lineage 9	This study
TA10_F54_I1	An isolate from TALE lineage 10	This study
TA11_F50_I1	An isolate from TALE lineage 11	This study
TA12_F55_I1	An isolate from TALE lineage 12	This study
TA13_F83_I1	An isolate from TALE lineage 13	This study
TA14_F82_I1	An isolate from TALE lineage 14	This study
TA15_F84_I1	An isolate from TALE lineage 15	This study
TA16_F86_I1	An isolate from TALE lineage 16	This study

S17_PP_5350’	*E. coli* S-17/pTE275_PP_5350’	This study
KT2440_PP_5350’	KT2440 PP_5350 (811-819del)	This study
S17_Δ*emrE*	*E. coli* S-17/pTE275_Δ*emrE*	This study
TA9_F60_I1_Δ*emrE*	A9_F60_I1 Δ*emrE*	This study
Plasmids		
pEX18GM	*sacB*-Gnt^R, a plasmid for the conjugation and a modified version of pEX18GM to have additional sequence.	[16]
pTE275_PP_5350’	*sacB*-Gnt^R, for the introduction of the PP_5350 mutation (811-819del) https://benchling.com/s/seq-94PMk93oehwWYf3iTzDA	This study
pTE275_Δ*emrE*	*sacB*-Gnt^R, for the deletion of *emrE,* https://benchling.com/s/seq-BUD8is3VWEEt72VNDWgJ	This study

[a]Number after “F” indicates the flask number which the strain was isolated from.

[b]See Supplementary Data 2 for detailed genotypes. Gnt^R indicates the gentamycin resistance gene.

Table S2. A list of oligonucleotides used in this study.

Name	Sequence (5' – 3')
PP_5350_F	TGCTTCAGGGCTTCGGCGGCTAGTCGACCCGTGCGGAAAA
PP_5350_B	AGGCTTTGAGCAATTGGTCGCTGGACATGCAGCTGTCGGA
PP_5350_V_F	TCCGACAGCTGCATGTCCAGCGACCAATTGCTCAAAGCCTCTAAG
PP_5350_V_B	TTTTCCGCACGGGTCGACTAGCCGCCGAAGCCCTGAAG
PP_5350_check_F	AAGTCGGCGCTCTGTGAAGC
PP_5350_check_B	GTCGCGTATTCACCCTAGCG
SacB_end_F	GCGAGACGAAAGGGCCTCG
EmrE_F1	TGCTTCAGGGCTTCGGCGGCGGGCCAAAGCTCGGTTTCCA
EmrE_B1	CAATGCCCAGCGGTCTTCGATTCGGCGCAGATGGCAATGG
EmrE_F2	CCATTGCCATCTGCGCCGAATCGAAGACCGCTGGGCATTG
EmrE_B2	AGGCTTTGAGCAATTGGTCGGGAATGCGTGCAGGGTTGGC
EmrE_V_F	GCCAACCCTGCACGCATTCCCGACCAATTGCTCAAAGCCTCTAAGAAAC
EmrE_V_B	TGGAAACCGAGCTTTGGCCCGCCGCCGAAGCCCTGAAG
EmrE_check_F	GATCAGGCTCATCTCGGCCAG
EmrE_check_B	GGTACTTCACGCCCTGATCG

Table S3. Summary of the ALE experiment results

Lineage	Target ionic liquid	Starting concentration (% w/v)	Initial growth rate[a]	Number of passages	Number of generations	Cumulative cell division (CCD, 10^{12})	Final concentration (% w/v)	Final growth rate[a]
ALE1	None	0	0.64 ± 0.09	84	583	2.88	0	0.77 ± 0.07
ALE2			0.61 ± 0.03	83	572	2.90	0	0.75 ± 0.05
ALE3			0.60 ± 0.08	85	580	2.80	0	0.87 ± 0.03
ALE4			0.47 ± 0.05	88	609	3.10	0	0.75 ± 0.08
TALE5	[TEOH][OAc]	0.5	0.38 ± 0.10	91	597	2.60	4.5	0.13 ± 0.02
TALE6			0.31 ± 0.03	80	544	2.59	4.1	0.11 ± 0.02
TALE7			0.32 ± 0.08	80	549	2.73	4.5	0.12 ± 0.04
TALE8			0.29 ± 0.02	83	563	2.79	4.1	0.13 ± 0.01
TALE9	[TEA][HS]	2	0.29 ± 0.04	60	402	2.18	7.2	0.17 ± 0.03
TALE10			0.36 ± 0.13	54	366	1.81	7.2	0.13 ± 0.05
TALE11			0.33 ± 0.06	50	335	1.64	7.2	0.15 ± 0.04
TALE12			0.32 ± 0.09	55	383	2.12	7.6	0.21 ± 0.05
TALE13	A 1:1 mix of [TEOH][OAC] and [TEA][HS]	1	0.44 ± 0.25	83	566	2.78	5.1	0.09 ± 0.01
TALE14			0.35 ± 0.09	82	548	2.49	4.7	0.12 ± 0.01
TALE15			0.33 ± 0.07	84	566	2.62	5.1	0.09 ± 0.01
TALE16			0.40 ± 0.12	86	567	2.57	4.7	0.11 ± 0.02

[a]The growth rates were measured using the automated liquid handling platform[17].

Table S4. Highly differentially expressed genes upon the addition of the ILs

Locus tag[a]	Gene	Description	Fold changes (FCs)
[TEOH][OAc]			
PP_0372	*aruC*	Acetylornithine aminotransferase 2	266.2
PP_4488		Conserved exported protein of unknown function	221.9
PP_4557		Conserved exported protein of unknown function	177.6
PP_0269		Putative glutamate synthase, large subunit	107.2
PP_1266		Putative fusaric acid resistance protein	82.0
PP_1264		Putative fusaric acid resistance protein	56.9
PP_2222		Conserved protein of unknown function	50.2
PP_5458		Conserved exported protein of unknown function	48.4
PP_1263		Putative fusaric acid resistance protein	46.9
PP_1743	*actP*-I	Acetate permease	-19.5
PP_2035	*benE*-I	Benzoate transport protein	-17.5
PP_3164	*benD*	1,6-Dihydroxycyclohexa-2,4-diene-1-carboxylate dehydrogenase	-14.6
PP_2037		Putative aldolase	-14.3
PP_1559		Holin	13.6
PP_3577	*fecI*	RNA polymerase, sigma 19 factor	12.2
PP_3163	*benC*	Benzoate 1,2-dioxygenase electron transfer	-10.9
PP_0883	*opdP*	Glycine-glutamate dipeptide porin	-10.7
PP_0799	*opdC*	Histidine-specific outer membrane porin D	10.4
PP_2036		Putative 4-hydroxy-tetrahydrodipicolinate synthase	-10.2
[TEA][HS]			
PP_3726		Enoyl-CoA hydratase	108.3
PP_3725		Putative acyl-CoA dehydrogenase	80.3
PP_2817	*mexC*	Multidrug efflux RND membrane fusion protein	60.6
PP_3724		Putative acyl-CoA synthetase	38.1
PP_4930	*emrE*	Putative small multidrug resistance protein	35.1
PP_3723	*aruI*	Putative 2-ketoarginine decarboxylase AruI	23.4
PP_5073		Conserved exported protein of unknown function	19.9
PP_5340	*aphA*	Acetylpolyamine aminohydrolase	14.6
PP_4738		Conserved exported protein of unknown function	13.7
PP_2818	*mexD*	Multidrug efflux RND transporter MexD	13.4
PP_4561	*csbD*	Stress response protein	12.9
PP_1750	*asnB*	Asparagine synthetase	12.7
PP_3732		Enoyl-CoA hydratase	10.9
PP_1185	*oprH*	Outer membrane protein H1	10.3

[a]Only differentially expressed genes (DEGs) whose FCs are larger than 10 were listed in this table. See Supplementary Data 2 for full lists of DEGs (FCs are greater than or equal to 2).

Table S5. Quantification of sugars and sugar byproducts

Ionic liquid	Final volume (mL)	Sugar (g/L)		Sugar byproduct (g/L)		Sugar yield[a] (% g sugar/g total sugar)	
		Glucose	Xylose	Furfural	5- Hydroxy methylfurfural	Glucose	Xylose
[TEOH] [OAc]	500	11.13 ± 0.47	6.61 ± 0.35	n.d.	n.d.	71.95 ± 3.06	70.90 ± 3.74
[TEA] [HS]	400	15.63 ± 1.31	1.79 ± 0.17	1.75 ± 0.08	0.35 ± 0.04	80.79 ± 6.75	15.38 ± 1.44

20 g of sorghum was pretreated using the ILs. Error bars indicate standard deviations of three measurements (n=3). n.d. not detectable (< 0.01 g/L)

[a]Glucan and xylan contents in sorghum were assumed to be 34.82% (g/g) and 20.44% (g/g), respectively (https://bioenergylibrary.inl.gov/Sample/BiomassInfo.aspx). The glucan and xylan weights were converted to the glucose and xylose weights by multiplying a factor of 1.111.

Supplementary Reference

1. D. Chatterji and A. K. Ojha, *Curr. Opin. Microbiol.*, 2001, **4**, 160–165.

2. J. M. Bergman, D. L. Hammarlöf, and D. Hughes, *PLoS One*, 2014, **9**, e90486.

3. E. T. Mohamed, A. Z. Werner, D. Salvachúa, C. Singer, K. Szostkiewicz, M. Jiménez-Díaz, T. Eng, M. S. Radi, A. Mukhopadhyay, M. J. Herrgård, S. W. Singer, G. T. Beckham, and A. M. Feist, *Metab Eng Commun*, submitted.

4. S. Chevalier, E. Bouffartigues, J. Bodilis, O. Maillot, O. Lesouhaitier, M. G. J. Feuilloley, N. Orange, A. Dufour, and P. Cornelis, *FEMS Microbiol. Rev.*, 2017, **41**, 698–722.

5. S. S. Fong, A. R. Joyce, and B. Ø. Palsson, *Genome Res.*, 2005, **15**, 1365–1372.

6. E. Blanco-Romero, M. Redondo-Nieto, F. Martínez-Granero, D. Garrido-Sanz, M. I. Ramos-González, M. Martín, and R. Rivilla, *Sci. Rep.*, 2018, **8**, 13145.

7. G. J. Bentley, N. Narayanan, R. K. Jha, D. Salvachúa, J. R. Elmore, G. L. Peabody, B. A. Black, K. Ramirez, A. De Capite, W. E. Michener, A. Z. Werner, D. M. Klingeman, H. S. Schindel, R. Nelson, L. Foust, A. M. Guss, T. Dale, C. W. Johnson, and G. T. Beckham, *Metab. Eng.*, 2020.

8. T. del Castillo, J. L. Ramos, J. J. Rodríguez-Herva, T. Fuhrer, U. Sauer, and E. Duque, *J. Bacteriol.*, 2007, **189**, 5142–5152.

9. M. Martínez-Gil, M. I. Ramos-González, and M. Espinosa-Urgel, *J. Bacteriol.*, 2014, **196**, 1484–1495.

10. E. Duque, J. de la Torre, P. Bernal, M. A. Molina-Henares, M. Alaminos, M. Espinosa-Urgel, A. Roca, M. Fernández, S. de Bentzmann, and J.-L. Ramos, *Environ. Microbiol.*, 2013, **15**, 36–48.

11. D. van den Broek, T. F. C. Chin-A-Woeng, G. V. Bloemberg, and B. J. J. Lugtenberg, *Microbiology,* 2005, **151**, 1403–1408.

12. M. M. Ochs, M. P. McCusker, M. Bains, and R. E. Hancock, *Antimicrob. Agents Chemother.*, 1999, **43**, 1085–1090.

13. S. Follonier, I. F. Escapa, P. M. Fonseca, B. Henes, S. Panke, M. Zinn, and M. A. Prieto, *Microb. Cell Fact.*, 2013, **12**, 30.

14. J. J. Rodríguez-Herva, E. Duque, M. A. Molina-Henares, G. Navarro-Avilés, P. Van Dillewijn, J. De La Torre, A. J. Molina-Henares, A. S. La Campa, F. A. Ran, A. Segura, V. Shingler, and J.-L. Ramos, *Environ. Microbiol. Rep.*, 2010, **2**, 373–380.

15. D. Szklarczyk, A. L. Gable, D. Lyon, A. Junge, S. Wyder, J. Huerta-Cepas, M. Simonovic, N. T. Doncheva, J. H. Morris, P. Bork, L. J. Jensen, and C. von Mering, *Nucleic Acids Res.*, 2019, **47**, D607–D613.

16. T. T. Hoang, R. R. Karkhoff-Schweizer, A. J. Kutchma, and H. P. Schweizer, *Gene*, 1998, **212**, 77–86.

17. R. A. LaCroix, B. O. Palsson, and A. M. Feist, *Appl. Environ. Microbiol.*, 2017, **83**.